39th AIAA Fluid Dynamics Conference & Exhibit, 22–25 June 2009, San Antonio, Texas

Detection of Wave Propagation by Nonstationary Cross-Correlation and Cross-Spectral Density Phase

A. Albert Ortiz*, and Frank K. Lu†

Aerodynamics Research Center, University of Texas at Arlington, Arlington, TX 76019, USA

The accurate determination of the speed of a propagating disturbance is important for a number of applications. A nonstationary cross-spectral density phase (NCSDP) technique was developed to provide a statistical estimate of the propagation time of sharp discontinuities such as steps or spikes that model shock or detonation waves. The uncertainty of the phase estimate is dependent on the coherence between the signals. For discrete implementation of the NCSDP technique, a "weighted-resetting-unwrap" of the phase angle was proposed to discard values of the coherence below a threshold value, that is, only the unwrapped phase angle above the threshold was accepted. In addition, an envelop function was used which improved the technique. The technique was found to be unsuitable for step disturbances but was more effective in estimating the time delay with a small standard deviation if the sharp disturbance also showed a rapid decay.

Nomenclature

CCC	Cross-correlation coefficient
$E[\ ]$	Expected value
f_s	Sampling frequency
n_d	Number of averages
N	Sample size
NCCC	Nonstationary cross-correlation coefficient
NCSDP	Nonstationary cross-spectral density phase
NCSDPE	Nonstationary cross-spectral density phase with envelope
R_{xy}	Nonstationary cross-correlation function
S_{xy}	One-sided frequency-time cross-spectral density
TOF	Time-of-flight
$\bar{u}$	Average wave propagation speed
Δf	$= f_s/N$, frequency increment
Δt	Time-of-flight of a disturbance between two sensors; also, sampling period
Δx	Distance between two sensors
ρ_{xy}	Nonstationary cross-correlation coefficient function
θ_{xy}	Phase angle
γ_{xy}	Coherence function
τ_{xy}	Time delay
σ	Standard deviation

*Graduate Research Assistant, Department of Mechanical and Aerospace Engineering.

†Professor, Department of Mechanical and Aerospace Engineering, Associate Fellow AIAA.

ω Angular frequency
$\hat{()}$ Estimate

I. Introduction

Determining the speed of a propagating disturbance is important for a number of applications. For example, the shock Mach number, so important for characterizing the perrformance of shock tubes and tunnels requires the measurement of the propagation time of shocks and other discontinuities.[1] In particular, the propagation of a detonation wave is of importance in fundamental studies of detonations[2] as well as in the development of pulse detonation engines.[3] The most common method for determining the wave propagation speed is by the time-of-flight (TOF) method in which the average wave propagation speed is defined by

$$\bar{u}_s \triangleq \Delta L/\Delta T. \tag{1}$$

where the distance between the sensors is known. The TOF method appears to be suitable for strong, distinct transient signals such as shock and detonation waves.[4–6] In situations where the signal is weak, the TOF method requires further treatment or may even have to be replaced by more powerful methods.

The TOF method is the most simplistic approach in determining the propagation time (also known as the delay time), but it can lead to poor estimates of uncertainty. The TOF method makes certain assumptions on the detection of the disturbance, primarily, that the disturbance results in a distinct signal. In reality, however, even such a signal is subject to some uncertainty due to transducer characteristics, thermal drift, finite transducer size, transducer mounting, the medium that the disturbance is propagating through and the data acquisition process itself such as the sampling rate. Therefore, the practical implementation of the TOF method can be subjective. This is because the shock front is not measured as a step rise, as in theory, but is spread over a small time interval due to the abovementioned factors. Different arbitrary criteria can, thus, be formulated for determining the shock arrival over a transducer. For example, the shock may be deemed to have arrived at the transducer when the signal rises above an arbitrary threshold, or when the signal is midway between arbitrarily defined upstream and downstream values. These criteria, which yield signal arrival times close to one another, are subjective. They may be unreliable if the error of the time estimate is comparable to ΔT. Such a situation may occur if the transducers are closely spaced or if the sampling rate is low. For the same record length, increasing the sampling rate does not fundamentally overcome this difficulty although it may reduce the uncertainty in the ΔT estimate.

To illustrate the arbitrariness of the TOF method for shock or detonation waves, consider the propagation of a fully-developed Chapman–Jouguet (CJ) detonation wave past two transducers in a stoichiometric oxy-hydrogen mixture initially at 2.01 atm, Fig. 1.[7] (Figure 1(a) includes other features, including a subsequent wave reflection, that will be described later.) The region where the pressure initially rises is enlarged and shown in Fig. 1(b). The symbols represent actual data, sampled at 100 kHz per channel with a simultaneous sample-and-hold system. Figure 1(b) shows that the two wave fronts $X(t)$ and $Y(t)$ are spread over a few data points. The double-headed arrows indicate possible pairs of data points for the TOF method, resulting in estimates of ΔT from 0.21 to 0.23 ms. The 0.02 ms uncertainty represents a ten percent error on the estimate of the velocity.

To evaluate the uncertainty, a nonstationary cross-spectral density phase (NCSDP) technique, which uses the entire spectra of both signals, was developed. This technique is an extension of classical cross-spectral phase techniques for stationary signals[9] and which is well established in the study of turbulence, acoustics and flow-induced vibrations, amongst others.[10–12] It should be noted that classical time and frequency domain statistical techniques such as used for turbulence studies assume stationarity and ergodicity. Both assumptions are not possible for transient phenomena such as those studied in the present work. The present work attempts to extend the application of cross-spectral techniques to transient phenomena characterized by a large discontinuity, either in the form of a step or a spike.

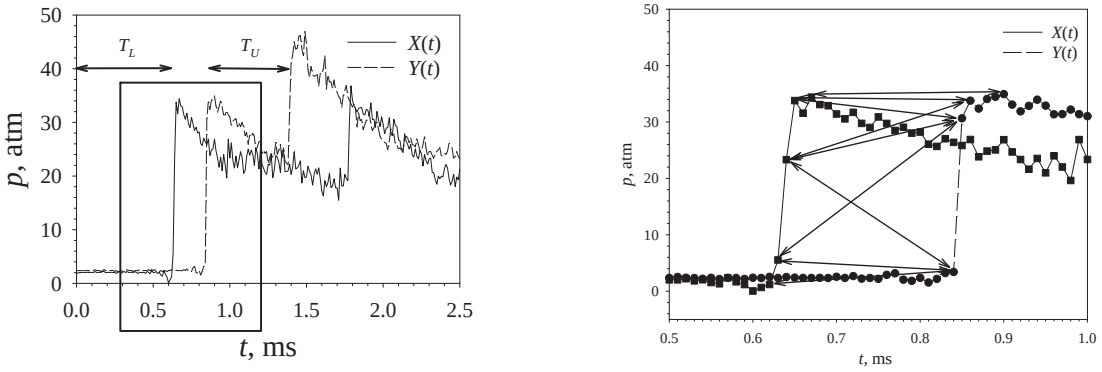

(a) Detonation wave propagating past two transducers.

(b) Enlargement of wave fronts.

Figure 1. Arbitrariness of the TOF method.

II. Determination of the Propagation Time

II.A. Nonstationary Cross-Correlation Technique

Background material is provided for a nonstationary cross-correlation technique that is related to the nonstationarly cross-spectral technique. A cross-correlation technique was previously proposed for determining the propagation time of shock and detonation waves.[7] The cross-correlation function (CCF) is a joint statistical property for a pair of random records that measures the fundamental properties shared by the pair of records in the time domain.[8,9] The CCF can be defined as

$$R_{xy}(\tau) \triangleq E[x(t)\, y(t+\tau)] = \int_{-\infty}^{\infty} x(t)\, y(t+\tau)\, dt \tag{2}$$

The CCF provides an estimate of the time delay between the given signals due to the propagation of a disturbance assuming stationarity.[9] The time delay estimate is provided by the maxima in the cross-correlation, which is the peak value for the CCF.

The CCF has to be modified for discrete data that are acquired at a finite rate for a finite period of time. Such a discrete, biased estimate CCF is given by

$$\widehat{R}_{xy}(i_\tau) = \frac{1}{N} \sum_{i=0}^{N-1} x(i)\, y(i+i_\tau), \quad i_\tau = -(N-1), -(N-2), \ldots, N-2, N-1 \tag{3}$$

where the time delays are determined by

$$\tau = i_\tau / f_s \tag{4a}$$

and

$$\Delta t = 1/f_s \tag{4b}$$

The estimate is said to be biased because of the finite window.

As an example, consider a pair of sine waves at 4 Hz, the second phase delayed by 90 deg, Fig. 2(a). This pair of sine waves has a known cross-correlation function which is also a sine wave that has a phase

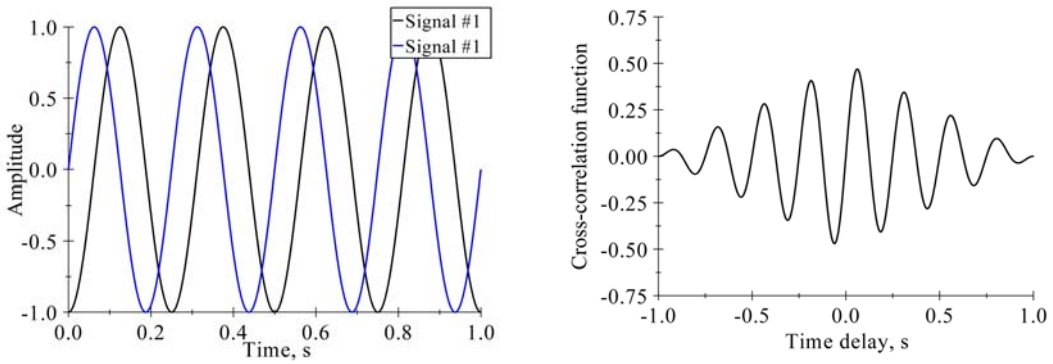

(a) Two 4 Hz sine functions, 90 deg out of phase.

(b) The biased cross-correlation function.

Figure 2. The biased cross-correlation function of two sine functions at 4 Hz, 90 deg out of phase.

equivalent to the time delay between the pair of signals.[9] The biased estimate of the CCF output for the two signals is shown in Fig. 2(b). Referring to Fig. 2(b), the CCF shows stronger correlations in the vicinity near zero time delay. The CCF also shows a decaying trend with increasing time delay due to the finite window. The peaks further from the maximum peak become broader, indicating weaker correlations. These features are unlike the analytical result if the two signals are infinitely long because the cross-correlation will then be an infinite sine function of constant amplitude between -1 and 1.

An unbiased estimate that corrects for the error near the edges of the window is

$$\widehat{R}_{xy}\left(i_\tau\right) = \frac{1}{N - |i_\tau|} \sum_{i=0}^{N-1} x\left(i\right) y\left(i + i_\tau\right), \quad i_\tau = -(N-1), -(N-2), \ldots, N-2, N-1 \tag{5}$$

The unbiased estimate of the CCF output of the signal pair in Fig. 2(a) is shown in Fig. 3. Unlike the biased estimate, the unbiased estimate of the CCF has uniform correlated peaks for the signals, as in the analytical solution of two infinite, continuous sine waves. Uncertainty for large time delays has been removed since the peaks do not broaden. The unbiased estimate of the time delay is also generally more accurate than the biased estimate.

The unbiased estimate of Eq. (5) is modified for *nonstationary* signals as

$$\widehat{R}_{xy}\left(l, i_\tau\right) = \frac{1}{N - |i_\tau|} \sum_{i=k}^{N-1} x\left(i\right) y\left(i + i_\tau\right), \quad l = 0, 1, \ldots, N-1 \tag{6}$$

where $M \leq N$ and l is the time index value. The nonstationary CCF relaxes the stationary assumption so that the time delay estimate is now achieved by averaging the peak values for the ensemble of CCF through different values of l. The time delay estimate is given by

$$\widehat{\tau} = \frac{1}{M} \sum_{i=0}^{M-1} \widehat{\tau}_{i,Max} \tag{7}$$

where $\widehat{\tau}_{i,Max}$ is the time delay value for the maximum correlated point for the given CCF. Previous work[7] provided three criteria for analyzing nonstationary events, namely,

1. Isolate the nonstationary event pair by not including any other events,

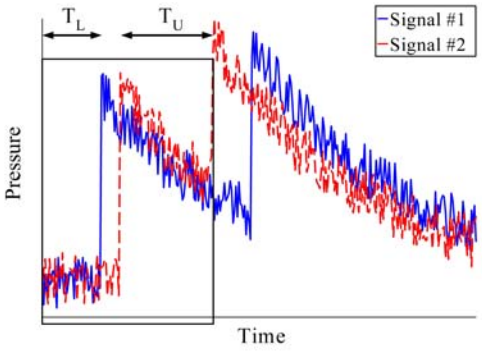

(a) Imposing a time-varying window based on the three criteria for nonstationary signals.

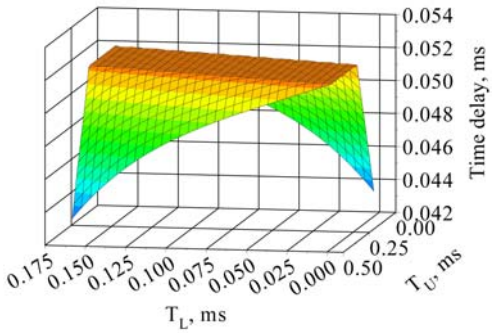

(b) The time delay surface from applying a nonstationary cross-correlation.

Figure 4. Illustrating the nonstationary cross-correlation technique.

2. Apply Chauvenet's acceptance criterion, and

3. Exclude the region where the nonstationary event does not occur for either signal.

The proposed NCCF was slightly modified to account for the time window and is given by[7]

$$\widehat{R}_{xy}\left(L,U,i_\tau\right)=\frac{1}{\left(U-L+1\right)-\left|i_\tau\right|}\sum_{i=L}^{U}x\left(i\right)y\left(i+i_\tau\right) \tag{8}$$

where L and U are the lower and upper time index value. An example of the time window with the proposed criteria is shown in Fig. 4(a). The figure shows a nonstationary event in the form of a propagating detonation wave which reflects off a wall and propagates in the opposite direction. The main window covering the nonstationary propagating event is shown by the rectangular window (black solid lines) with the lower and upper time limits. The lower and upper time limits are used to define all the possible windows for the NCCF. The time delay that is obtained is represented by a surface as shown in Fig. 4(b).

As a further example, consider the passage of a detonation wave past a pair of pressure transducers spaced 4 in. (101.6 mm) apart. The signals were sampled at 240 kHz and are shown in Fig. 5(a). The figure shows both signals capturing the detonation wave propagation as a nonstationary event. Both signals exhibit a spike with an oscillating exponential decay.

The nonstationary CCF is normalized with respect to the mean square values for the pair of signals to form the cross-correlation coefficient (CCC):

$$\widehat{\rho}_{xy}\left(L,U,i_\tau\right)\triangleq\frac{\widehat{R}_{xy}\left(L,U,i_\tau\right)}{\sqrt{\widehat{R}_{xx}\left(L,U,0\right)\widehat{R}_{yy}\left(L,U,0\right)}} \tag{9}$$

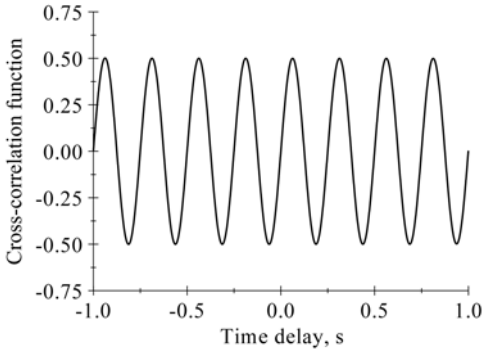

Figure 3. The unbiased estimate of the CCF of the signal pair in Fig. 2(a).

The CCC has a range from -1 to 1, where the sign dictates if the signals are negatively or positively correlated. A CCC value of 1 signifies a perfect positive correlation whereas a value of zero provides no correlation between the pair of records. The nonstationary

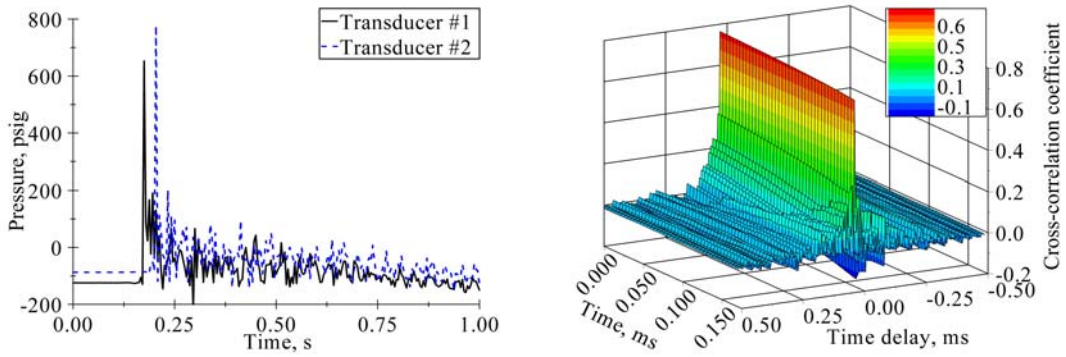

(a) Pressure history for a detonation wave propagating by two transducers.

(b) Nonstationary CCC for a constant U value.

Figure 5. Example of the nonstationary cross-correlation technique applied to a propagating detonation wave.

CCC output of Fig. 5(a) is shown in Fig. 5(b). In this example, the nonstationary CCC is obtained for a varying time window that has a moving lower limit and a constant upper limit, unlike the example of Fig. 4. The maximum value of the CCC is about 0.8, indicating a strong correlation. The signal is not better correlated due to the presence of high-frequency disturbances. The figure also shows that the CCC has a well-defined peak when the lower time limit is at a maximum value. However, as the lower time index approaches the disturbance, the peak value decreases slightly with an increase of the values surrounding the maximum CCC. This can increase the uncertainty in the time delay estimate.

II.B. Non-Stationary Cross-Spectral Density Phase Technique

A spectral technique, known as the non-stationary cross-spectral density phase (NCSDP) technique, that is based on the cross-correlation function is proposed. The cross-spectral density is obtained by applying the Fourier transform to the cross-correlation function and is given by

$$S_{xy}(f) = \int R_{xy}(\tau)\, e^{-j2\pi f\tau} d\tau \tag{10a}$$

$$S_{xy}(f) = |S_{xy}(f)|\, e^{-j\theta_{xy}(f)} \tag{10b}$$

where the phase angle θ_{xy} is related to the time delay τ via

$$\theta_{xy}(f) = -2\pi f \tau(f) \tag{11}$$

For nondispersive signals such as shock and detonation waves, the time delay remains constant for all frequencies; thus, the phase angle remains linear throughout the spectrum.

The double-sided nonstationary cross-spectral density function,[9] which is a slight alteration of the original cross-spectral density function of Eq. (10a), is given by

$$W_{xy}(f,t) \triangleq \int R_{xy}(\tau,t)\, e^{-j2\pi f\tau} d\tau \tag{12}$$

Equation (12) is discretized to yield

$$\widehat{W}_{xy}(k,L,U) = \sum_{i_\tau=-(N-1)}^{N-1} \widehat{R}_{xy}(L,U,i_\tau) \exp\left(-j\frac{2\pi k i_\tau}{N}\right) \tag{13}$$

Since the discrete Fourier transform algorithm, namely, the fast Fourier transform, starts its lower bound index at zero instead of $-(N-1)$, the discrete version of the NCSDP has to be altered to satisfy this condition. The modified discrete version of the nonstationary cross-spectral density function is thus written as

$$\widehat{W}_{xy}(k,L,U) = \sum_{m=0}^{2N-2} \widehat{R}_{xy}(L,U,m) \exp\left(-j\frac{2\pi km}{N}\right) \tag{14}$$

where

$$m = i_\tau + N - 1 \tag{15}$$

The phase angle can then be computed by

$$\widehat{\theta}_{xy}(k,L,U) = \tan^{-1}\left\{\frac{\Im\left[\widehat{W}_{xy}(k,L,U)\right]}{\Re\left[\widehat{\mathcal{W}}_{xy}(k,L,U)\right]}\right\} \tag{16}$$

where the quadrant is determined according to the sign of the imaginary and real components.

Similar to the stationary case, the cross-spectral density can be written in complex polar notation as

$$\widehat{W}_{xy}(k,L,U) = \left|\widehat{W}_{xy}(k,L,U)\right| e^{-j\widehat{\theta}_{xy}(k,L,U)} \tag{17}$$

The time delay can then be related to the phase angle for a nondispersive propagation as

$$\widehat{\theta}_{xy}(k,L,U) = -2\pi km\Delta f\Delta t \tag{18}$$

which after substitution for m is

$$\widehat{\theta}_{xy}(k,L,U) = 2\pi k\Delta f\left[i_\tau\Delta t + (N-1)\Delta t\right] \tag{19}$$

Substitution of $f = k\Delta f$ and Eqs. (4a) and (4b) into the discrete phase angle in Eq. (19) forms

$$\widehat{\theta}_{xy}(f,t) = -2\pi f\left[\widehat{\tau} + \frac{(N-1)}{f_s}\right] \tag{20}$$

which can be used for comparing with the analog phase angle.

The discretized version of the phase angle has additional terms that are not present in the analog version in Eq. (11). These additional terms present a problem in the time delay estimate. For simplicity, a case with no time delay is considered and the phase angle reduces to

$$\widehat{\theta}_{xy}(f,t) = -2\pi f\left(\frac{N-1}{f_s}\right) \tag{21}$$

The discrete version of the phase angle is

$$\widehat{\theta}_{xy}(k,L,U) = -2\pi k\Delta f\left(\frac{N-1}{f_s}\right) = -2\pi k\frac{f_s}{N}\left(\frac{N-1}{f_s}\right) \tag{22a}$$

$$= -2\pi k\left(\frac{N-1}{N}\right), \qquad k = 0,1,\ldots,N-1 \tag{22b}$$

In the limit as the sample size approaches infinity, the phase angle estimate approaches a multiple of 2π. This represents an equivalent result for an autocorrelation function which is the simple case of no time delay.

But, with a positive time delay, the phase angle will exceed 2π, creating an uncertainty of 2π in the phase estimate, known as *phase aliasing*. Due to phase aliasing, the time delay estimate is impossible to determine directly. An example of phase aliasing is shown in Fig. 6 in which the sampling rate is 500 kHz, the sample size is 10 000 and the time delay is 1 ms. The true phase uses Eq. (20) and the discrete phase uses Eq. (11). In this figure, the actual phase angle (solid black line) is an infinite sawtooth function. The discrete phase-aliased representation of this data is shown as a red dashed-line with markers. Since the discrete phase angle is sampled at a rate that exceeds the range of the phase angle $-\pi \leq \widehat{\theta}_{xy} \leq \pi$, the true phase-to-frequency relationship is lost. Unfortunately, increasing the sampling rate or the amount of samples acquired cannot prevent phase aliasing.

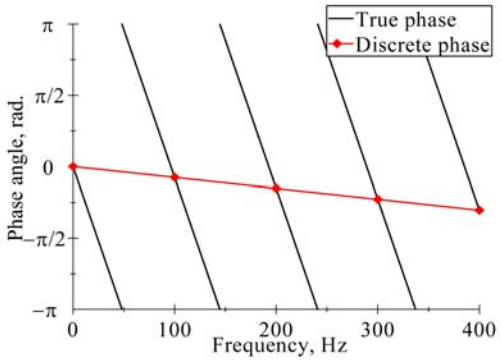

Figure 6. An example of phase aliasing that is caused by the discretizing the equations.

However, a zoom transform can be used to overcome phase aliasing. The phase–frequency relationship remains the same with the application of a zoom transform, but the zoom transform now improves the frequency resolution. It is recommended that the spectral resolution be improved by a factor of four. This recommendation is based on using the maximum time delay value and setting the phase equation equal to π. The process for determining the factor is derived from Eq. (20) and is as follows:

$$\widehat{\theta}_{xy} = 2\pi k \Delta f \left(f_{ratio}\right) \left(\frac{N}{f_s} + \frac{N-1}{f_s}\right) = 2\pi k f_{ratio} \left(\frac{f_s}{N}\right) \left(\frac{2N-1}{f_s}\right) \tag{23a}$$

$$= 2\pi k f_{ratio} \left(\frac{2N-1}{N}\right) \approx 4\pi k f_{ratio} \tag{23b}$$

Setting the phase angle and the frequency index equal to π and one respectively in Eq. (23b) yields

$$f_{ratio} \triangleq \Delta f_{zoom} / \Delta f = 1/4 \tag{24}$$

where Δf_{zoom} is the frequency resolution of the zoom transform.

II.B.1. Phase Uncertainty

The discretized phase angle in Eq. (20) is an exact solution, which only occurs in an ideal case with a very high SNR with the signals being highly coherent. Since this is not the case most of the time, a way of estimating the phase uncertainty needs to be developed and is given by[8]

$$\Delta\widehat{\phi}_{xy}\left(f\right) \approx \sin^{-1}\left[\frac{\sqrt{1-\gamma_{xy}^2\left(f\right)}}{\left|\gamma_{xy}\left(f\right)\right|\sqrt{2n_d}}\right] \tag{25}$$

According to Eq. (25), the phase uncertainty can be reduced by having highly coherent signals or by using a large number of averages. Table 1 shows several numbers of averages for various coherence values. The table shows that signals with low coherence values require a large number of averages to improve the phase estimate. For example, if the desired phase uncertainty is set to 0.033 radians, a coherence value of 0.9 can achieve the phase uncertainty with 50 averaged records. A much larger number of records (200 in this example) are needed for the exact same uncertainty in the phase angle at a lower coherence value of 0.7.

Table 1. The phase uncertainty in radians for various coherence values

	Number of averages (n_d)				
γ^2	1	10	50	100	200
0.1	2.121	0.671	0.300	0.212	0.150
0.3	1.080	0.342	0.153	0.108	0.076
0.5	0.707	0.224	0.100	0.071	0.050
0.7	0.463	0.146	0.065	0.046	0.033
0.9	0.236	0.075	0.033	0.024	0.017
1.0	0.000	0.000	0.000	0.000	0.000

II.B.2. Coherence Function

The uncertainty in the phase estimate is dependent on the coherence between the signals. The coherence function is a measure of degree of correlation between the signals in the frequency domain[13] and can be written as

$$\gamma_{xy}(f) = \sqrt{\frac{|S_{xy}(f)|^2}{S_{xx}(f)\,S_{yy}(f)}} \tag{26}$$

that is $0 \leq \gamma_{xy} \leq 1$ throughout the spectrum. A coherence value of zero indicates pure noise that is uncorrelated while a value of unity signifies perfect correlation. Typically, the coherence of the signals is less than unity due to noise present in the given measurement, resolution bias errors in the spectral estimates, a nonlinear relation between the given signals, or the second sensor receiving other inputs that were not previously present for the initial sensor.[8] An example of a coherence function for the experimental data of Fig. 5(a) is shown in Fig. 7. It can be noted in that frequencies near the structures resonant frequency have highly incoherent signals due to the amplification of the noise.[14]

Uncertainty exists in determining the phase when the coherence is less than unity. For the present analysis, a threshold for rejecting the portions of the spectrum was set for coherence of less than or equal to 50 percent. This threshold is shown in Fig. 7 for the data of Fig. 5(a).

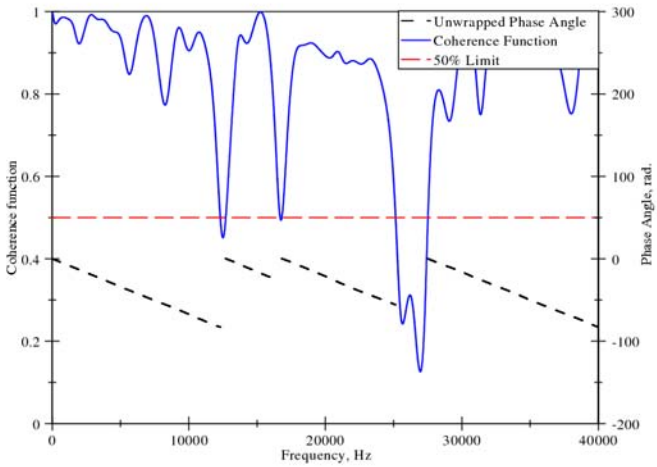

Figure 7. Phase angle being unwrapped according to the coherence of the signals and subject to a coherence limit 50 percent for the data of Fig. 5(a).

II.B.3. Weighting Function

A weighting function is needed for transforming the correlation function from the time to the frequency domain. The weighting function is used mainly for two reasons. It is needed to reduce the spectral leakage that degrades the coherence between the signals, and to smooth the edges that may be erratic due to the limited information near the edge of the defined lower and upper bounds.

II.B.4. Unwrapping Phase

In an analog signal, the phase angle does not need to be unwrapped because it has an adequate amount of samples before a phase jump. For the discrete phase version, leaving the phase angle wrapped leads to few samples before a phase jump which increases the error in the estimate for determining the slope of the phase angle. The difference in the slopes between the analog and discrete version is shown in Fig. 7. The discretized version has a much steeper slope than the analog version for the same time delay. The samples for the discrete version also decrease depending on the coherence of the signals at a particular frequency. For this reason, a "weighted-resetting-unwrap" of the phase angle method is proposed. As far as the authors are aware, this method has not been attempted, at least for shock and detonation waves.

The weighted-resetting-unwrap of the phase angle method consists of unwrapping the phase angle continuously till the coherence value drops below the coherence limit. Once the limit has been crossed the phase angle is reset and offset to return the initial phase angle at zero. All of the values below the coherence threshold are discarded. An example of the result of applying this method is provided in Fig. 7. Referring to Fig. 7, the phase angle (dashed black line) is unwrapped multiple times and is reset back to zero every time the coherence (solid blue line) of the signals drops below the coherence limit (dashed red line). With a less tolerant coherence limit, more portions of the phase angle will be reset with smaller samples due to the increase of discarding of values below the coherence limit.

II.B.5. Linear Fit

A linear least-squares fit was applied to extract the phase–frequency relationship in order to determine the time delay. Since there exists the possibility of multiple, disconnected portions of the unwrapped phase as shown in Fig. 7, which shows four unwrapped portions, a weighting scheme was used based on the number of samples for a given segment. For this method, the 0–12 and 28–40 kHz portions in Fig. 7 would be weighted the most as they contain a larger portion of frequencies above the coherence limit, while the 13–15 kHz portion would have less weight in the overall determination of the phase-frequency relationship since it contains the least amount of samples. This process is continued for each time step, which generates a single phase–frequency relationship for an individual time step.

II.B.6. Time Delay

Determining the time delay between the given signals with Eq. (19) is problematic for signals with poor coherence. A more appropriate method would utilize the phase–frequency relationship for the autospectral density functions in determining the time delay. The time delay can be determined by computing the average difference between the phase-frequency relationships for the cross-spectral and autospectral density functions. This method does not require previous knowledge of the sampling properties and is given by

$$\widehat{\widetilde{\tau}}_{xy}(t) = \frac{1}{2}\left[\left(\left.\frac{d\theta}{d\omega}\right|_{xx} - \left.\frac{d\theta}{d\omega}\right|_{xy}\right) + \left(\left.\frac{d\theta}{d\omega}\right|_{yy} - \left.\frac{d\theta}{d\omega}\right|_{xy}\right)\right] \tag{27}$$

The estimate in Eq. (27) is now used to determine the time delay for each individual time step for the nonstationary signals. Chauvenet's criterion is then applied to eliminate outliers in order to prevent bad estimates that are highly influenced by the edge of the window near the disturbance.

II.C. Non-Stationary Cross-Spectral Density Phase Envelope Technique

The nonstationary cross-spectral density phase envelope (NCSDPE) technique is very similar to the NCSDP method. The difference between the two methods is that the NCSDPE method utilizes the envelope correlation coefficient (ECC) that was proposed in Bendat and Piersol.[9] The ECC is given by

$$\widehat{\rho}_{uv}\left(L, U, i_\tau\right) = \widehat{\rho}^2_{xy}\left(L, U, i_\tau\right) + \widehat{\widetilde{\rho}}^{\,2}_{xy}(L, U, i_\tau) \tag{28}$$

where ρ_{xy} is the NCCC and $\tilde{\rho}_{xy}$ is the Hilbert transformation of the NCCC. Similar to the NCCC in the NCSDP method, the ECC is transformed into the frequency domain where the remaining steps are the same. The utilization of the ECC method has an advantage over the use of the NCCC method as it provides more distinct peaks for the maximum correlated values.

III. Results and Discussion

The NCSDP and NCSDPE techniques were tested with a number of model functions, similar to tests performed on the NCCF,[7] namely:

- Unit step functions $X(t)$ and $Y(t)$ both with SNR = 8–32 and with $Y(t)$ delayed by $\tau_M = 50$;
- A unit step function $X(t)$ at $t = 0$ with SNR = 16, and a step function $Y(t)$ at $\tau_M = 50$ with an amplitude of $A = 2^{-2}$ – 2^3 and SNR = 16;
- Exponentially decaying functions $X(t) = e^{-bt/100}$ and $Y(t) = e^{-b(t-\tau_M)/100}$, where $b = 2^{-2}$ – 2^2 and SNR = 16 for both functions, and $\tau_M = 50$;
- Linearly decaying functions $X(t) = 1 - ct/100$ and $Y(t) = 1 - c(t - \tau_M)/100$, where $c = 2^{-2}$ – 2^2 and SNR = 16 for both functions, and $\tau_M = 50$.

Uniformly distributed white noise was added to the model functions. The SNR was determined by

$$\text{SNR (dB)} = 10 \log_{10} P_{signal}/P_{noise} \tag{29}$$

where P_{signal} and P_{noise} represent the power of the signal and noise respectively. For all the functions, the sample size was set to 1001 and the time step $\Delta t = 1$. Since these tests were to examine the dependence of NCSDP and NCSDPE upon data characteristics, the routine to vary the limits of the integration window $[T_L, T_U]$ was not included for expediency. The lower limits were set to $T_L = 0$ and 400 while the upper limits were set to $T_U = 600$ and 1001. These functions are displayed in Fig. 8.

The corresponding estimated means and standard deviations of the time delay using the NCSDP method are shown in Table 2 for coherence thresholds of 50, 60 and 75 percent. Large errors are seen in the estimate of the mean that is also subjected to large estimated standard deviations for the step function. But, for either the exponential or linear decays, good estimates of the time delay is obtained if these decays are sharp, with the estimate increasing with decreasing coherence. A summary of the results from Table 2 for the NCSDP method follows:

- **Step, varying SNR.** The results for the varying SNR step functions show that increasing noise level has an adverse effect on the mean and standard deviation estimates in producing seriously erroneous results for the former and large values for the latter. Extraordinarily large standard deviation estimates were obtained for the three coherence limits. These difficulties render the NCSDP method useless for a step function even for low noise conditions.
- **Step, varying amplitude.** Similar conclusions as above can be derived.
- **Exponential decay.** The results from the exponential decaying functions provide some insight into the capabilities of the NCSDP method. Improved estimates for both the mean and the standard deviation were obtained for fast decay rates, $b \geq 1$. In other words, the NCSDP method appears well suited for "peaky" signals. However, the method is still generally inaccurate except for the peakiest signals.
- **Linear decay.** The results for the linear decaying functions show a similar trend as for the exponential decaying functions. For fast decay rates, $c \geq 1$, the mean estimates were very accurate, with a small standard deviation. Similar to the exponential decay, the slower decay rates provided worse results since the functions approached a step-like appearance. A possible reason that the linear decay provides better results than the exponential decay for a given decay rate is due to the higher power of the noise P_{noise} in the signal at a given decay rate to satisfy the given SNR. THe linear decay function also decays faster to zero.

Generally, the time delay estimates and standard deviation are improved with increasing the coherence limit. The NCSDP method also requires that the function being analyzed is decaying at a relatively fast rate to provide reasonable results.

Results from the NCSDPE method are shown in Table 3. The results show a vast improvement over the NCSDP method and are summarized as follows:

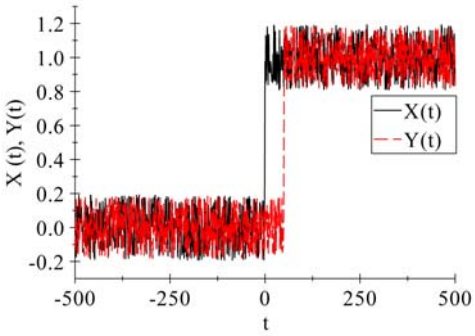

(a) Step function; various SNR.

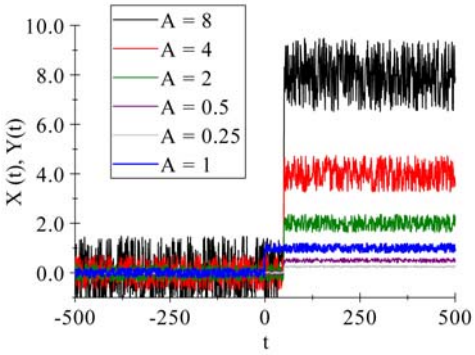

(b) Step function; various amplitudes for $Y(t)$, both with SNR = 16.

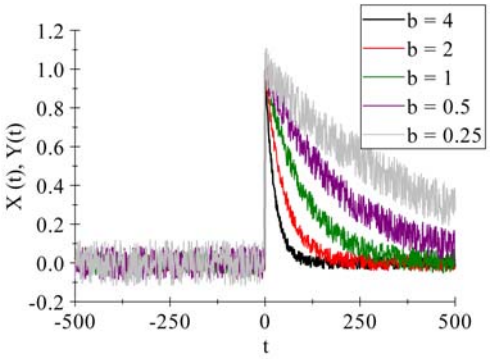

(c) Exponential decay with SNR = 16 (only $X(t)$ is shown).

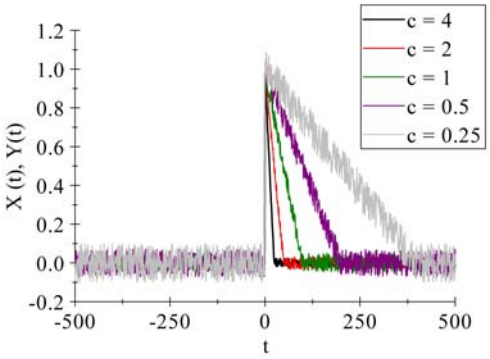

(d) Linear decay with SNR = 16 (only $X(t)$ is shown).

Figure 8. Model functions.

Table 2. NCSDP time delay values for model functions of Fig. 8

Coherence	50%		60%		75%	
	Step change with different signal-to-noise ratio					
	μ_t	σ_t	μ_t	σ_t	μ_t	σ_t
SNR = 32 dB	57.0	47.9	55.7	53.4	49.9	49.7
16 dB	90.4	41.0	78.6	41.4	58.5	35.3
8 dB	51.0	23.2	46.9	24.1	45.7	27.4
	Step change with different amplitude					
	μ_t	σ_t	μ_t	σ_t	μ_t	σ_t
$A = 0.25$	97.5	52.1	93.2	51.3	78.9	40.9
0.5	91.0	54.4	84.9	47.0	60.2	42.5
2	107.4	43.4	103.9	38.6	83.6	39.5
4	79.9	42.7	71.0	42.2	58.0	37.9
8	93.5	50.4	89.5	52.4	78.1	48.2
	Exponential decay					
	μ_t	σ_t	μ_t	σ_t	μ_t	σ_t
$b = 4$	49.8	0.0	49.8	0.0	49.8	0.0
2	29.6	5.5	27.7	5.6	49.6	1.5
1	49.9	12.3	47.6	10.7	45.3	10.7
0.5	34.9	31.8	35.2	28.9	39.9	32.8
0.25	67.7	43.0	35.7	39.5	25.1	34.6
	Linear decay					
	μ_t	σ_t	μ_t	σ_t	μ_t	σ_t
$c = 4$	50.0	0.0	50.0	0.0	50.0	0.0
2	50.0	0.0	50.0	0.0	50.0	0.0
1	49.8	4.1	49.9	4.0	53.1	3.7
0.5	40.6	36.8	27.0	34.4	34.5	29.3
0.25	29.8	39.1	32.8	40.5	33.6	38.8

Table 3. NCSDPE time delay values for model functions of Fig. 8

Coherence	0%		50%		60%		75%	
	Step change with different signal-to-noise ratio							
	μ_t	σ_t	μ_t	σ_t	μ_t	σ_t	μ_t	σ_t
SNR = 32 dB	50.1	0.0	50.1	0.0	50.1	0.0	50.1	0.0
16 dB	40.1	7.4	39.4	7.4	38.9	7.2	53.6	0.3
8 dB	14.2	10.1	42.5	18.5	63.9	2.2	40.5	4.2
	Step change with different amplitude							
	μ_t	σ_t	μ_t	σ_t	μ_t	σ_t	μ_t	σ_t
$A = 0.25$	35.6	8.8	43.3	7.3	49.9	1.4	54.6	0.6
0.5	40.1	10.1	41.1	8.4	46.9	7.6	49.7	8.7
2	39.1	6.8	42.3	5.7	43.6	4.5	51.8	0.3
4	35.0	8.6	39.0	7.6	39.8	7.7	51.3	0.3
8	47.6	10.9	50.2	8.1	50.3	8.0	53.8	0.7
	Exponential decay							
	μ_t	σ_t	μ_t	σ_t	μ_t	σ_t	μ_t	σ_t
$b = 4$	49.8	0.0	49.8	0.0	49.8	0.0	49.8	0.0
2	50.0	0.0	49.9	0.0	50.0	0.0	50.1	0.0
1	49.7	0.1	50.0	0.0	50.0	0.0	50.0	0.0
0.5	50.1	0.2	49.9	0.7	49.9	0.7	50.3	0.4
0.25	47.6	3.6	51.1	1.7	50.3	0.5	49.9	0.1
	Linear decay							
	μ_t	σ_t	μ_t	σ_t	μ_t	σ_t	μ_t	σ_t
$c = 4$	50.0	0.0	50.0	0.0	50.0	0.0	50.0	0.0
2	50.1	0.0	50.1	0.0	50.1	0.0	50.1	0.0
1	49.9	0.0	49.9	0.0	49.9	0.0	50.0	0.0
0.5	50.0	0.9	50.0	0.0	50.0	0.0	50.0	0.0
0.25	46.5	3.8	48.3	1.8	48.7	1.5	50.1	0.1

- **Step, varying SNR.** The results for the varying SNR step functions show vastly improved estimates of the mean and extremely small standard deviations when the noise level is low. The mean was not properly estimated at the higher coherence limits when the SNR is poor.
- **Step, varying amplitude.** Similar conclusions as above can be derived.
- **Exponential decay.** Very good results for the mean and either negligible or very small values of the standard deviation were obtained for all decay rates, particularly at high coherence.
- **Linear decay.** The best estimates for the mean with the least values of the standard deviation were obtained for linearly decaying functions. A possible reason is due to the reduced power of the noise P_{noise} in the signal due to the faster decay of the linear functions.

Based on the above observations, the NCSDPE method proves to be superior to the NCSDP method as it is able to provide a better time delay estimate with small standard deviations even at a lower coherence limit.

IV. Conclusions

A nonstationary cross-spectral density phase technique was developed to provide a statistical estimation for the propagation time of a transient event, specifically a discontinuity in the form of a step or a spike. For discrete implementation of the NCSDP technique, a "weighted-resetting-unwrap" of the phase angle was proposed to discard values of the coherence below a threshold value, that is, only the unwrapped phase angle above the threshold was accepted. A zoom transform with a frequency ratio of 1/4 was used to overcome phase aliasing and also to improve the frequency resolution.

Erroneous estimates of the mean and large standard deviations were obtained when the signal-to-noise ratio is poor and when the coherence is set too low. The technique performed extremely poorly for step discontinuities but is better suited for sharply defined spikes. However, by modifying the technique through inclusion of an envelope function, a vast improvement is achieved that makes the technique viable for rapidly decaying, nonstationary signals even in the presence of a large amount of noise.

V. Acknowledgements

This work is partly funded by the National University of Singapore via Research Collaboration Agreement No. TL/AE/2008/01.

References

[1]Lu, F.K. and Wilson, D.R., "Detonation Driver for Enhancing Shock Tube Performance," *Shock Waves*, Vol. 12, No. 6, 2003, pp. 457-468.

[2]Li, J., Lai, W.H., Chung, K. and Lu, F.K., "Uncertainty Analysis of Deflagration-to-Detonation Run-Up Distance," *Shock Waves*, Vol. 14, No. 5–6, 2005, pp. 413–420.

[3]Kailasanath, K., "Recent Developments in the Research on Pulse Detonation Engines," *AIAA Journal*, Vol. 41, No. 2, 2003, pp. 145–159.

[4]Ishii, K., Kataoka, H. and Kojima, T., "Initiation and Propagation of Detonation Waves in Combustible High Speed Flows," *Proceedings of the Combustion Institute*, Vol. 32, 2009, pp. 2323-2330.

[5]Kontis, K., An, R., Kounadis, D. and Zare-Behtash, H., "Head-On Collision of Shock Wave Induced Vortices with a Cylinder and a Sphere," *International Journal of Heat and Fluid Flow*, Vol. 29, No. 5, 2008, pp. 1380-1392.

[6]Rakitin, A.E. and Starikovskii, A.Y., "Mechanisms of Deflagration-to-Detonation Transition Under Initiation by High-Voltage Nanosecond Discharges," *Combustion and Flame*, vol. 155, No. 1–2, 2008, pp. 343–355.

[7]Lu, F.K., Ortiz, A.A., Li, J.-M., Kim, C.H. and Chung, K.-M., "Detection of Shock and Detonation Wave Propagation by Cross Correlation," *Mechanical Systems and Signal Processing*, Vol. 23, No. 4, 2009, pp. 1098–1111.

[8]Bendat, J.S. and Piersol, A.G., *Engineering Applications of Correlation and Spectral Analysis,* 2nd ed., John Wiley & Sons, Inc., New York, 1993.

[9]Bendat, J.S. and Piersol, A.G., *Random Data Analysis and Measurement Procedures*, 3rd ed., John Wiley & Sons, Inc., New York, 2000.

[10]Ciappi, E., Magionesi, F., De Rosa, S., Franco, F., "Hydrodynamic and Hydroelastic Analyses of a Plate Excited by the Turbulent Boundary Layer," *Journal of Fluids and Structures*, Vol. 25, No. 2, 2009, pp. 321–342.

[11]Bailey, S.C.C., Hultmark, M., Smits, A.J. and Schultz, M.P., "Azimuthal structure of turbulence in high Reynolds number pipe flow," *Journal of Fluid Mechanics*, Vol. 615, 2008, pp. 121–138.

[12]Hall, J.W., Hall, A.M., Pinier, J.T. and Glauser, M.N., "Cross-Spectral Analysis of the Pressure in a Mach 0.85 Turbulent Jet," *AIAA Journal*, Vol. 47, No. 1, 2009, pp. 54–59.

[13]Norton, M.P. and Karczub, D.G., *Fundamentals of Noise and Vibration Analysis for Engineers*, 2nd ed., Cambridge University Press, Cambridge, UK, 2003, pp. 543–547.

[14]Inman, D.J., *Engineering Vibration*, 2nd ed., Prentice Hall, Englewood Cliffs, New Jersey, 2001.